Frequency evaluation of UTC(NPL) by NPL-Sr1 for the period MJD 59639 to 59669

National Physical Laboratory

March 20, 2023

The secondary frequency standard NPL-Sr1 and an optical frequency comb were used to evaluate the frequency of UTC(NPL) over a period of 30 days from MJD 59639 to MJD 59669 (1st March 2022 – 31st March 2022). The Sr optical lattice clock operation covers 60.5% of the total measurement period. The result of the evaluation is reported in table 1 and is made using the CCTF 2021 recommended frequency value for the $5s^2\ {}^1S_0$ – $5s5p\ {}^3P_0$ unperturbed optical transition in ^{87}Sr: 429 228 004 229 872.99 Hz with a relative standard uncertainty of $u_{\mathrm{Srep}} = 1.9 \times 10^{-16}$ [1].

Period of estimation	y(UTC(NPL)−NPL-Sr1) $/10^{-16}$	u_{A} $/10^{-16}$	u_{B} $/10^{-16}$	$u_{\mathrm{A/Lab}}$ $/10^{-16}$	$u_{\mathrm{B/Lab}}$ $/10^{-16}$	u_{Srep} $/10^{-16}$	Uptime
MJD 59639–59669	9.72	0.004	0.22	4.98	0.56	1.9	60.5%

Table 1: Results of the evaluation of UTC(NPL) by NPL-Sr1.

1 Measurement configuration

NPL-Sr1 was operated as described in reference [2], with the exception of some changes described in section 2 below. The 698 nm clock laser was pre-stabilized to a local reference cavity and then phase-locked via a fibre-based optical frequency comb to another more stable laser at 1064 nm. A feedback loop acting on an acousto-optic modulator (AOM) kept the clock laser frequency in resonance with the ^{87}Sr clock transition.

Following a change in the reference maser for UTC(NPL) in January 2021, and a subsequent redistribution of reference frequency signals within NPL in February 2021, the optical frequency comb was no longer referenced to UTC(NPL), but instead to a separate maser reference HM6.

The frequency ratio between the ^{87}Sr clock transition and HM6 was calculated from the comb measurements of the 698 nm ultrastable laser and the AOM frequency corrections. The frequency ratio was determined as the midpoint of a weighted linear fit to the NPL-Sr1/HM6 ratio data. The time offset between HM6 and UTC(NPL) was continually measured by an SR620 time interval logger. By taking the derivative of this time offset we determined the mean frequency difference between the two signals over the evaluation period. This was then combined with the frequency comb measurements to obtain the frequency ratio between the ^{87}Sr clock transition and UTC(NPL). HM6 was not steered during this evaluation period.

Systematic effect	Correction / 10^{-18}	Uncertainty / 10^{-18}
BBR chamber	4986.2	7.0
BBR oven	0.5	0.5
Quadratic Zeeman	240.7	0.3
Lattice	0.0	20.0
Collisions	0.0	3.8
Background gas	5.3	5.3
DC Stark	0.016	0.016
Probe Stark	1.0	0.4
Servo Error	0.0	2.0
Total Correction	5233.7	22.3
Gravitational redshift	-1215.0	2.7
Total including gravitational redshift	4018.7	22.4

Table 2: Uncertainty budget of the NPL-Sr1 lattice clock for this evaluation period. Reported uncertainties correspond to 68% confidence intervals.

2 NPL-Sr1 evaluation

Type A uncertainty

The type A uncertainty u_A is the statistical contribution from the frequency instability of NPL-Sr1. This was estimated based on a white frequency noise component of $4.5 \times 10^{-16}/\sqrt{\tau}$, extrapolated to the duration of the evaluation period.

This is an improvement compared to the earlier reports covering the periods MJD 58659–58679 ($5 \times 10^{-16}/\sqrt{\tau}$), MJD 58454–58459 ($8 \times 10^{-16}/\sqrt{\tau}$ and MJD 57904–57919 and MJD 57929–57934 ($2 \times 10^{-15}/\sqrt{\tau}$). The improvement is a direct result of improvements made to the 1064 nm laser to which the 698 nm clock laser is stabilised. The stability was evaluated by interleaved measurements.

Type B uncertainty

The type B uncertainty u_B is the sum in quadrature of the systematic uncertainty of NPL-Sr1 and the uncertainty of the gravitational redshift relative to the conventionally adopted reference potential $W_0 = 62\ 636\ 856.0\ \mathrm{m^2 s^{-2}}$.

The systematic frequency corrections and uncertainty budget for NPL-Sr1 for the period of this report are given in table 2. The geopotential value for NPL-Sr1 is taken from [3].

Changes to the uncertainty evaluation presented in reference [2] are described below.

Blackbody radiation

In this report we use an updated dynamic correction coefficient for blackbody radiation, reported in reference [4]. This leads to an increase of 4×10^{-18} in the total BBR correction for our operational conditions close to 300 K, compared to the value obtained using the previous coefficient.

Quadratic Zeeman

For this evaluation, we returned to using a stretched state splitting similar to that used in reference [2], following an increase for the reports covering the periods MJD 58454–58459 and MJD 58659–

58679. However, we continue to use the updated value for the quadratic Zeeman shift coefficient of $-2.456(3) \times 10^{-7}$ Hz^{-1} [5].

Background Gas

As for the previous evaluation covering the period MJD 58659–58679, we use an updated coefficient for the background gas collisional shift of $(-3.0 \pm 0.3) \times 10^{-17}/\tau$, where τ is the $1/e$ vacuum-limited trap lifetime [6]. Assuming hydrogen is the dominant gas in our system we arrive at a shift of -5.3×10^{-18} based on lattice trapped lifetime measurements of 5.7 s (re-evaluated after installation of the lattice enhancement cavity in August 2018). However, since the gas composition is only assumed and the lifetime measurement may be reduced by parametric heating in the lattice trap we assign an uncertainty equal to the shift.

Collisions

In August 2018, a lattice enhancement cavity was implemented on NPL-Sr1. As a result, the trapping waist is considerably larger than in reference [2] (153 µm compared to 65 µm). The shift due to cold collisions is therefore expected to be lower than previously, but the uncertainty is conservatively estimated to be the same as before.

Lattice

Lower than normal atom number during this evaluation period prevented a full evaluation of the lattice shift following our normal procedure. Full evaluations performed for the evaluation periods MJD 58454–58459 and MJD 58659–58679 resulted in uncertainties of 4×10^{-18} and 3.0×10^{-18} respectively, and for this evaluation period adjustment of the lattice frequency back to the extrapolated magic condition followed similar procedures as previously. Interleaved measurements at high and low trap depths were carried out to constrain the shift, but because a full evaluation was not possible we apply no correction and assign a conservative uncertainty to this shift of 2×10^{-17}.

3 Frequency comparison

Type A uncertainty

The uncertainty $u_{\mathrm{A/Lab}}$ arises mainly from the dead time in the comparison between HM6 and NPL-Sr1, and includes both a deterministic correction due to maser drift and a stochastic contribution (table 3).

The stochastic contribution was estimated by a method described in reference [7]. This involves a Monte-Carlo approach where the frequency noise of HM6 is simulated and a value calculated for

Contribution	Uncertainty / 10^{-18}
$u_{\mathrm{A/Lab}}$[Deterministic]	65
$u_{\mathrm{A/Lab}}$[Stochastic]	494
$u_{\mathrm{A/Lab}}$[HM6-UTC(NPL)]	11
$\boldsymbol{u_{\mathrm{A/Lab}}}$**[Total]**	498

Table 3: A breakdown of the uncertainties included in $u_{\mathrm{A/Lab}}$.

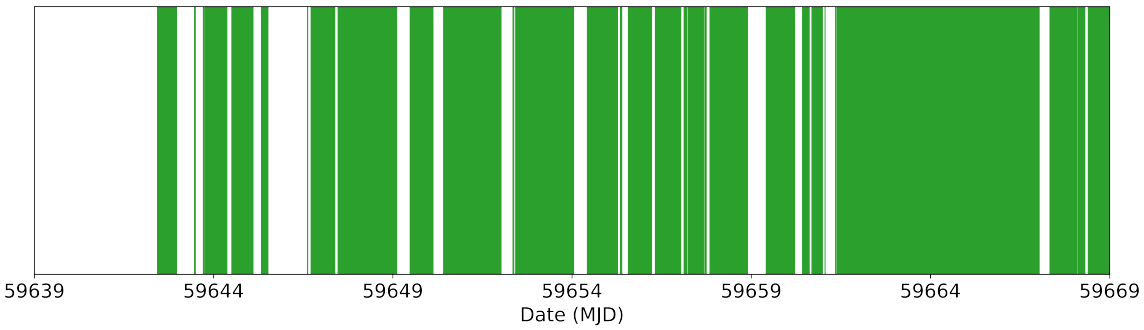

Figure 1: Uptime of NPL-Sr1 over the evaluation period (green regions).

the offset between the mean frequency during the uptime periods and the mean frequency during the whole evaluation period. The simulation was repeated 1000 times, with the standard deviation of the offsets providing an estimate for the frequency uncertainty arising from the dead times in the operation of NPL-Sr1.

The maser noise model used comprised white phase noise of $1.25 \times 10^{-13}/\tau$, white frequency noise of $4.90 \times 10^{-14}/\sqrt{\tau}$, a flicker frequency floor of 1.25×10^{-15} and a random-walk frequency component of $2.55 \times 10^{-19}\sqrt{\tau}$. In addition, maser HM6 exhibits diurnal frequency fluctuations that were estimated as an additional noise process proportional to the sum of two sinusoids in the simulated noise, with amplitudes 2.5×10^{-15} and 3.0×10^{-15} and periods 3×10^4 s and 8.64×10^4 s respectively. These values were derived from measurements of HM6 by NPL-Sr1 our caesium fountain primary frequency standard NPL-CsF2.

For this evaluation period, NPL-Sr1 had an uptime of 60.5%, distributed as shown in figure 1.

The SR620 time interval logger that links HM6 to UTC(NPL) introduces an additional contribution to $u_{\mathrm{A/Lab}}$, which is computed from the statistical spread of the time interval measurements.

Type B uncertainty

The most significant contribution to the uncertainty $u_{\mathrm{B/Lab}}$ is the distribution of the 10 MHz signal from HM6 to the frequency comb laboratory, and the subsequent synthesis in that laboratory of an 8 GHz signal against which the repetition rate of the frequency comb was measured. Potential phase fluctuations were monitored using a loop-back comparison as described in reference [2], and their contribution to the uncertainty estimated from the instability of these fluctuations over the evaluation period.

The SR620 time interval logger that links HM6 to UTC(NPL) also contributes to $u_{\mathrm{B/Lab}}$. This contribution is estimated based on the specification of the instrument.

Contribution	Uncertainty / 10^{-18}
$u_{\mathrm{B/Lab}}$[Distribution]	49
$u_{\mathrm{B/Lab}}$[HM6-UTC(NPL)]	27
$\boldsymbol{u_{\mathrm{B/Lab}}}$**[Total]**	56

Table 4: A breakdown of the uncertainties included in $u_{\mathrm{B/Lab}}$.

References

[1] Consultative Committee for Time and Frequency (CCTF), "Recommendation PSFS-2 from the 22nd meeting (session II – online)," (2022).

[2] R. Hobson, W. Bowden, A. Vianello, A. Silva, C. F. A. Baynham, H. S. Margolis, P. E. G. Baird, P. Gill, and I. R. Hill, "A strontium optical lattice clock with 1×10^{-17} uncertainty and measurement of its absolute frequency," Metrologia **57**, 065026 (2020).

[3] F. Riedel, A. Al-Masoudi, E. Benkler, S. Dörscher, V. Gerginov, C. Grebing, S. Häfner, N. Huntemann, B. Lipphardt, C. Lisdat, E. Peik, D. Piester, C. Sanner, C. Tamm, S. Weyers, H. Denker, L. Timmen, C. Voigt, D. Calonico, G. Cerretto, G. A. Costanzo, F. Levi, I. Sesia, J. Achkar, J. Guéna, M. Abgrall, D. Rovera, B. Chupin, C. Shi, S. Bilicki, E. Bookjans, J. Lodewyck, R. L. Targat, P. Delva, S. Bize, F. N. Baynes, C. F. A. Baynham, W. Bowden, P. Gill, R. M. Godun, I. R. Hill, R. Hobson, J. M. Jones, S. A. King, P. B. R. Nisbet-Jones, A. Rolland, S. L. Shemar, P. B. Whibberley, and H. S. Margolis, "Direct comparisons of European primary and secondary frequency standards via satellite techniques," Metrologia **57**, 045005 (2020).

[4] C. Lisdat, S. Dörscher, I. Nosske, and U. Sterr, "Blackbody radiation shift in strontium lattice clocks revisited," Phys. Rev. Research **3**, L042036 (2021).

[5] T. Bothwell, D. Kedar, E. Oelker, J. M. Robinson, S. L. Bromley, W. L. Tew, J. Ye, and C. J. Kennedy, "JILA SrI optical lattice clock with uncertainty of 2.0×10^{-18}," Metrologia **56**, 065004 (2019).

[6] B. X. R. Alves, Y. Foucault, G. Vallet, and J. Lodewyck, "Background Gas Collision Frequency Shift on Lattice-Trapped Strontium Atoms," in *2019 Joint Conference of the IEEE International Frequency Control Symposium and European Frequency and Time Forum (EFTF/IFC)* (IEEE, Orlando, FL, USA, 2019) pp. 1–2.

[7] D.-H. Yu, M. Weiss, and T. E. Parker, "Uncertainty of a frequency comparison with distributed dead time and measurement interval offset," Metrologia **44**, 91 (2007).